

Internal Structure of the Green Lake 5 Rock Glacier, Colorado Front Range, USA

M. Leopold,^{1*} M.W. Williams,² N. Caine,² J. Völkel¹ and D. Dethier³

¹ Technische Universität München, WZW, Geomorphology and Soil Science, Freising, Germany

² University of Colorado, INSTAAR & Department of Geography, USA

³ Williams College, Dept of Geoscience, USA

ABSTRACT

Information about the internal structure of rock glaciers is needed to understand their reaction to ongoing climate warming. Three different geophysical techniques—shallow seismic refraction, ground-penetrating radar (GPR) and electrical resistivity tomography—were used to develop a detailed subsurface model of the Green Lake 5 rock glacier in the Colorado Front Range, USA. Below a thin zone of fine sediments and soils (0.7–1-m thickness; 0–20 kΩm and 320–370 m s⁻¹), a 1–3-m thick zone with low p-wave velocities (790–820 m s⁻¹) and high electrical resistivity (20–100 kΩm) is interpreted as the ice-free, blocky active layer with large void spaces. The data corroborate strong reflections of the GPR signals which travel at this depth at 0.11 m ns⁻¹. A third layer that extends from depths of 1–3 m to about 5 m is characterised by lower electric resistivities (5–20 kΩm) and has lower electromagnetic wave velocities (0.65 m ns⁻¹), representing unfrozen, finer and wetter sediments. At around 5-m depth, the measured physical parameters change drastically (vp = 3200–3300 m s⁻¹, 50–150 kΩm, vGPR = 0.15 m ns⁻¹), showing an ice-rich permafrost zone above the bedrock. This model of the internal structure was used to evaluate an existing hydrological flowpath model based on the hydrochemical properties of water outflow from the rock glacier. Copyright © 2011 John Wiley & Sons, Ltd.

KEY WORDS: rock glacier; ground-penetrating radar; seismic refraction; electrical resistivity tomography; hydrology

INTRODUCTION

The potential hydrologic significance of rock glaciers has been frequently overlooked (Millar and Westfall, 2008). It is possible that ice stored in these landforms may provide significant amounts of water storage and runoff during the summer in high-elevation catchments (Corte, 1976; Clow *et al.*, 2003). Recently, Azócar and Brenning (2010) and Brenning and Azócar (2010) described the hydrological significance of rock glaciers in the Dry Andes. These hydrologic roles may become increasingly important under future, warmer climates, as surface snow and ice fields melt and mountain permafrost active layers thaw earlier in the season (Harris *et al.*, 2003, 2009; Leopold *et al.*, 2010; Li *et al.*, 2008; Millar and Westfall, 2008).

If we are to increase our predictive capacity for how the hydrology of rock glaciers may change in response to a changing climate, we need to improve our understanding of their internal structure and the hydrologic flowpaths within and through them (Williams *et al.*, 2006). Knowledge of the internal structure of rock glaciers is limited as it is very

difficult to drill boreholes and sections are rare (see overview in Haeberli *et al.*, 2006). There remains much research to be done on the role of ice in rock glaciers, particularly as to whether there is a central core of pure ice, an ice-rock mixture, or some combination of these (Barsch, 1996).

In recent years, geophysical methods have been used with increasing frequency to derive subsurface information in permafrost areas, including surveys on rock glaciers (Hilbich *et al.*, 2009; Schrott and Sass, 2008; Hauck and Kneisel, 2008; Ikeda, 2008; Kneisel *et al.*, 2008). While these methods provide data on the internal structure and even the ice/water content of rock glaciers (e.g. Hausmann *et al.*, 2007), there is still little known about the hydrology of most of these forms and only a few studies to date have defined outflow rates (Krainer and Mostler, 2002). Moreover, many of the previous ground-penetrating radar (GPR) studies on rock glaciers were conducted during winter because of easier logistics and improved antennae-ground contacts with a snow cover (Berthling and Melvold, 2008), but thereby preventing the evolution of flowpaths through the rock glacier from being observed during the melt season.

Williams *et al.* (2006, 2007) developed a conceptual model of the hydrology of rock glaciers using the

Received 15 September 2009

Revised 14 November 2010

Accepted 14 November 2010

* Correspondence to: M. Leopold, E-mail: leopold@wzm.tum.de

geochemical and isotopic content of outflow water. A three-component hydrograph separation, using end-member mixing analysis from the rock glacier at Green Lake 5 (RG5) in the Colorado Front Range, suggested that snow was the dominant water source in June, soil water the dominant water source in July and internal ice melt the dominant source in September. From the hydrological data, it was inferred that the rock glacier has an internal ice core surrounded by interstitial ice within a coarse debris mantle (Figure 1). Because water samples are easy to collect and analyse, the approach developed by Williams *et al.* (2006, 2007) could have broad applicability to help increase our understanding of the hydrologic source waters and flowpaths of rock glaciers and how those might change in response to a changing climate. It is therefore important to know if their model is robust.

In this paper we develop a model of the structure of RG5, the rock glacier studied by Williams *et al.* (2006), through the use of shallow seismic refraction (SSR), GPR and electrical resistivity tomography (ERT). We compare this to the conceptual model of Williams *et al.* (2006) and discuss the implications for future hydrological studies.

STUDY SITE

A detailed site description is given by Williams *et al.* (2006), thus we present only the basics. The glacial Green Lakes Valley is situated at the northwestern edge of the Colorado Front Range (40°03'N and 105°35'W) with a maximum elevation of 4048 m at the Continental Divide and a minimum elevation of 3500 m. Green Lakes Valley is a Long-Term Ecological Research (LTER) network site, as

well as one of the Boulder Creek Critical Zone Observatory (BC-CZO) study areas. The valley is subject to a continental high-mountain climate. A 54-year climate record on Niwot Ridge (D1), about 1 km northeast of the rock glacier, shows a mean annual temperature of -3.7°C (Greenland, 1989; Williams *et al.*, 1996) with mean annual precipitation of 1000 mm, of which about 80 per cent falls as snow (Caine, 1996). The combined evidence of ground and air temperatures, surface landforms, topography and ground cover suggests that permafrost might underlie 80% or more of the Green Lakes Valley (Janke, 2005; 2007).

RG5 is a lobate rock glacier (Outcalt & Benedict, 1965) at an elevation of 3600 m on the north-facing side of Kiowa Peak (4000 m a.s.l.). The rock glacier, which is of Holocene age (White, 1976, 1981; Caine, 2001), covers an area of 8 ha. Parts of its surface are vegetated with grasses and sedges whereas others are covered by bare sediments/soils. Boulders on the surface of RG5 are angular to subangular, vary in size from cobbles to boulders several metres in diameter and are primarily gneissic rock (Williams *et al.*, 2006). The rock glacier consists of two lobes (Figure 2): a more active western lobe with a very steep front ($>35^{\circ}$), which was moving at a rate of about 2.0 cm yr^{-1} in the late 1960s (White, 1971), and a more inactive eastern lobe with a less steep front (*ca.* 33°). Its activity in recent years has been confirmed by field observations.

There is a small outflow stream at the base of the most active area of the rock glacier. Measuring its discharge is very difficult, because, like most rock glaciers, all of the flow is through multiple small channels within bouldery debris (Kraimer and Mostler, 2002; Williams *et al.*, 2006). We collected water samples for chemical and isotopic analyses from the outflow stream, and although we were not

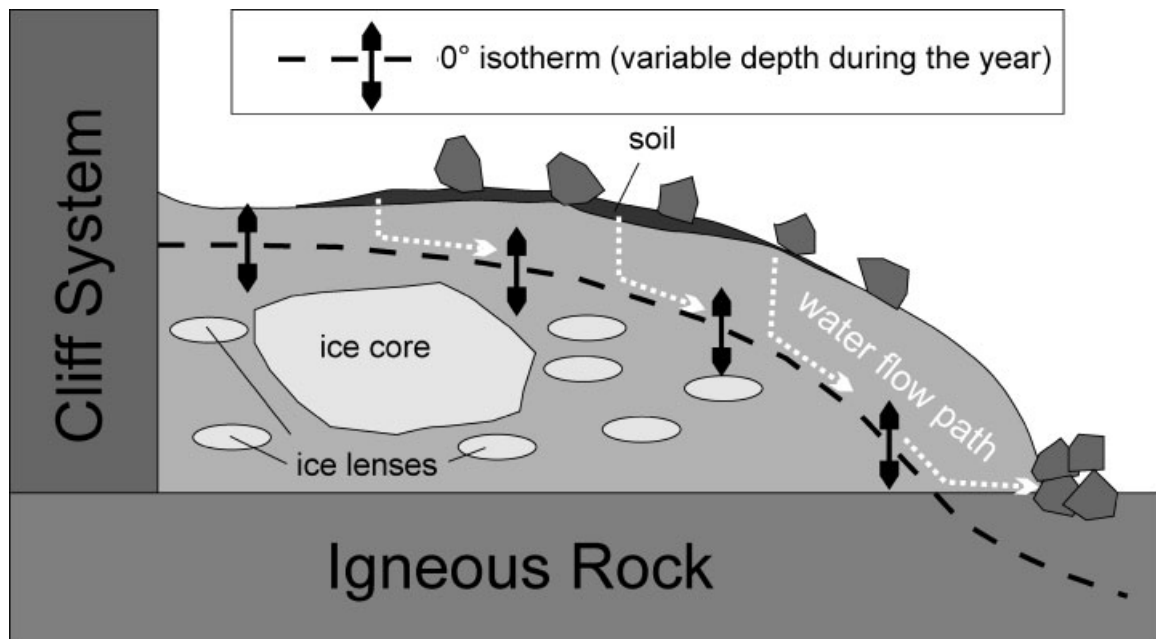


Figure 1 Conceptual model of the Green Lake 5 rock glacier based on water sources and flowpaths (after Williams *et al.*, 2006).

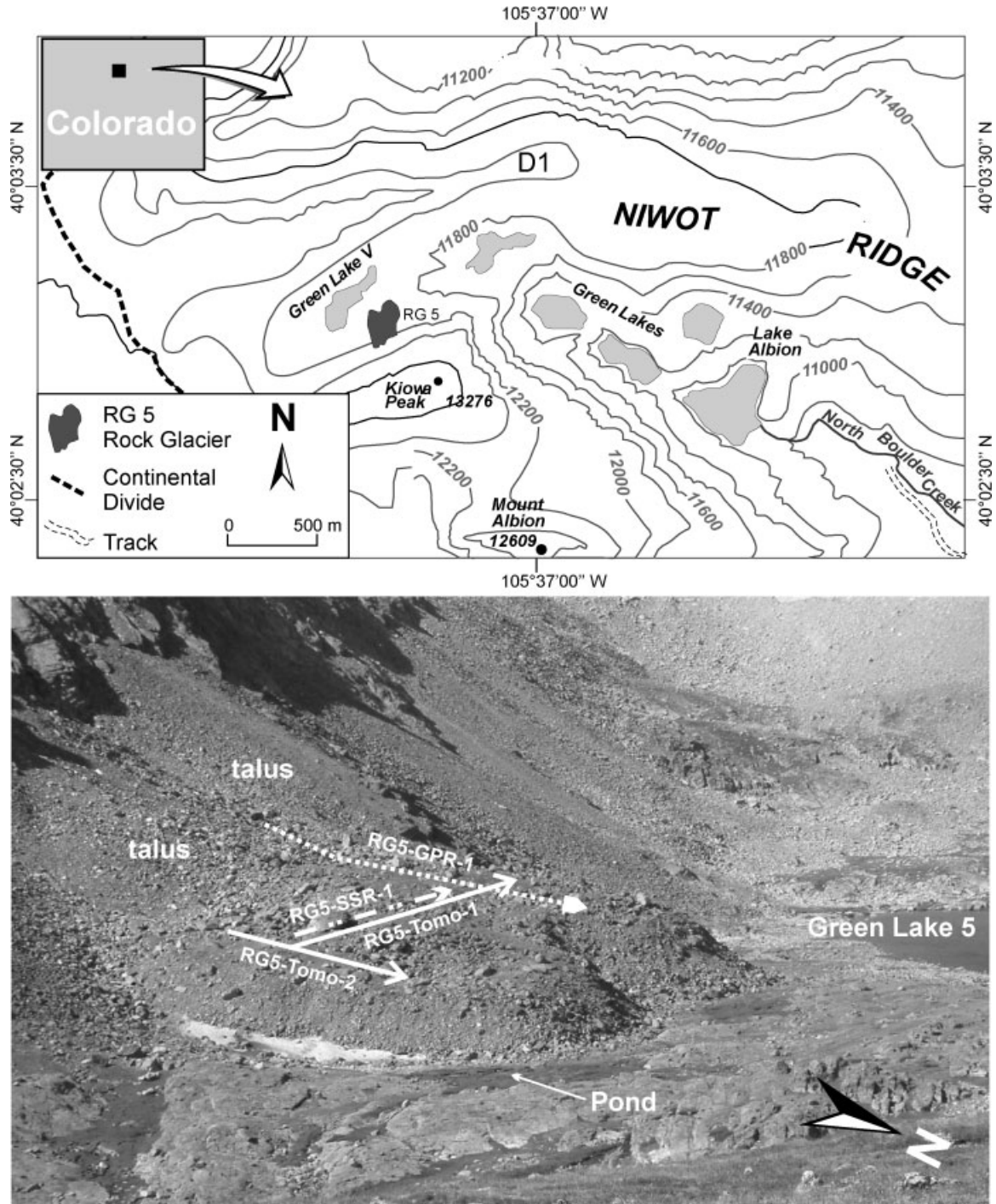


Figure 2 Study site. Inset top left shows the location of the study site in relation to the rectangular Colorado state boundaries. The site is situated within the Colorado Front Range close to the continental divide. The Green Lake 5 rock glacier (RG5) is located at the north flank of Kiowa Peak (4046 m). D1 = location of weather station D1. Photograph shows RG5 with location of the geophysical lines. GPR = Ground-penetrating radar; SSR = shallow seismic refraction; Tomo-1 and Tomo-2 = electrical resistivity tomography models 1 and 2.

able to measure discharge, we noted wide fluctuations in water level over short time intervals. Details of sample collection, isotopic and chemical analyses, and detection limits and precision are given in Williams *et al.* (2006, 2007).

METHODS

Three different geophysical methods were used to portray the internal structure of RG5. First, SSR uses acoustic waves that travel with specific speeds through different kinds of material. In general, acoustic waves travel faster in dense materials. We intended to use SSR to differentiate between blocky material with interstitial air, water or ice and the bedrock. Second, GPR uses electromagnetic waves that are pulsed into the ground. Depending on the conductivity and dielectric properties of the materials, the subsurface produces reflections and refractions of the electronic signal that can be traced and stored in a computer. This technique is highly sensitive to changes in the water-ice-air content. Third, ERT measures differences in electrical resistivity of the subsurface, which also reflects the material and water-ice content. The data from all techniques can be interpreted together to obtain a subsurface model of the physical properties of a rock glacier.

SSR

We used a 12-channel Smartseis seismic system from Geometrics California, USA, with a geophone spacing of 2.5 m (line length 27.5m) and a sledgehammer as energy source. As a result of harsh weather conditions in July 2007, we collected only one 27.5-m line with a forward and reverse shot point. We locally removed the upper organic layers to ensure the best contact of the geophones and the steel striker plate with the ground. Stacking was five times at each shot

Table 1 Filter sequence applied to ground-penetrating radar lines as shown in Figure 4.

Applied filter sequence
1. Import (import as new 32 bit floating point file)
2. Subtract-mean (dewow at 10 ms)
3. Time zero (correct max. phase / groundwave to time zero)
4. Background removal 2-D filter (a calculated mean trace is subtracted from each trace)
5. Time cut off (two way travel time was set to 450 ns)
6. Gain control (linear gain in y-direction)
7. Static correction (a topography was applied by the shift of start times in x-direction)

Table 2 Summary of electrical resistivity tomography lines on Green Lake 5 rock glacier (RG5).

Name of line	No. of electrodes	Spacing [m]	Array type	No. of data points
RG5-Tomo-1	50	1	Dipole-Dipole	578
RG5-Tomo-2	39	2	Dipole-Dipole	384

point to reduce background noise and to increase the energy due to compression of the upper few centimetres of the rather loose surface (Krummel, 2005). ReflexW 5.0 from Sandmeier scientific software (Karlsruhe, Germany) was used to calculate travel times and to develop a subsurface velocity model. Wavefront inversion and subsequent network/raytracing were applied to the travel times (see Hofmann and Schrott, 2003 or Leopold *et al.*, 2008a).

GPR

GPR has been used to study the internal structures of rock glaciers since the 1980s (see Degenhardt *et al.* 2003; Hausmann *et al.*, 2007; Maurer and Hauck, 2007; Degenhardt, 2009). Our radar lines were collected on 25 July 2005 using a portable RAMAC CU II GPR system from MALÅ Geosystems, Skolgatan, Sweden. We used 50- and 100-MHz antennae to obtain two-dimensional (2D) profiles. In this paper, we present a line collected with the 50-MHz antennae as this frequency consistently gave the best results. During the field survey the antennae were spaced 2 m apart, parallel to each other and perpendicular to the direction of the survey line. We collected data every 0.5 m and each trace was stacked 16 times. Common midpoint (CMP) surveys were carried out in several fairly flat and smooth areas to measure local electromagnetic wave velocity with a step size of 10 cm and a frequency of 100 MHz. Reflex W 5.0 was again used to process and display the GPR data using the filter sequence shown in Table 1. The protocol for this filter sequence for GPR processing is based on previous research in this kind of environment (e.g. Degenhardt, 2009; Hausmann *et al.*, 2007; Leopold *et al.*, 2008b). Interpretation was based on visual inspection of the reflection pattern following Neal (2004).

ERT

A multi-electrode system 4punktlight hp (Lippmann Geophysikalische Messgeräte, Schaufling, Germany) was used to collect 2D DC resistivity tomography profiles (Table 2). Fine-grained sediments and water were used to reduce contact resistance resulting in values between 2 and 10 k Ω , which is low for rock glaciers and therefore ensures good-quality data (cf. Hauck and Kneisel, 2008). As a result of the low contact resistances, we chose a dipole-dipole array, which results in higher resolution of the upper few metres compared to other array types (e.g. Wenner). We measured with a frequency of 5 Hz and 0.1–5.0 mA. Each point was measured between two and six times, depending on the variability of the results (3% limit).

A 2D-model interpretation of the apparent resistivities was performed using the software RES2DINV 3.55.18 (Loke and Barker, 1995). Topography was added and different inversion techniques (least squares, robust) were used to compile specific resistivity models. After five iterations, the models reached the desired convergence limit of 3.0 per cent. It started with a damping factor of $\lambda_0 = 0.15$ and ended with $\lambda_{\min} = 0.03$. This yielded absolute errors of 6.3 per cent to 3.3 per cent for robust inversions and root-mean-square errors of 7.9 per cent to 5.8 per cent for least-squares inversions, which are within the suggested value range of data misfit (Hauck and Vonder Mühll, 2003).

For each line we calculated the depth of investigation (DOI) index following Oldenburg and Li (1999) and Marescot *et al.* (2003) to determine which areas of the model are sensitive to the measured physical properties. Reference models were performed with resistivities of 0.1 and 10 times background resistivity, which was calculated

as the average of the apparent resistivities resulting in a two-sided difference (Oldenburg and Li, 1999). We developed scaled DOI values using models with three times depth of the estimated maximum DOI with a vertical-horizontal damping factor relationship of 1:1. Results were normalised to unity and the threshold value, used to determine areas below which the data are no longer sensitive to the physical properties of the subsurface, was set to 0.2 following Hilbich *et al.* (2009).

RESULTS

SSR

Picking first breaks for the several traces was challenging for some geophones and we used an interpolation between clearly identifiable picks (Figure 3). Travel times were

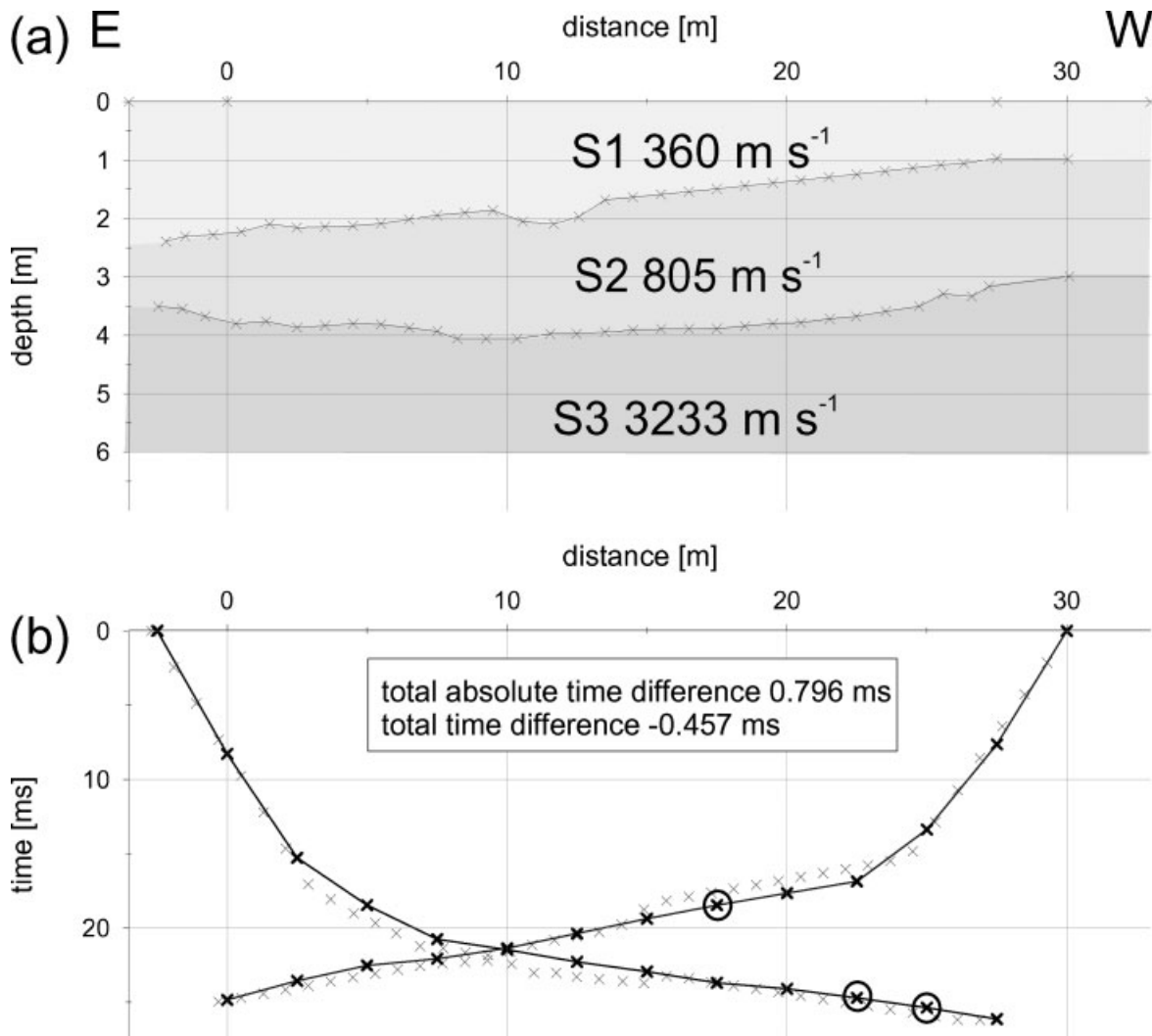


Figure 3 P-wave velocity model of a section at the Green Lake 5 rock glacier after wavefront inversion. The model was carefully adapted after the application of network raytracing techniques. Picks surrounded by a circle indicate interpolated travel time points.

inverted using wavefront inversion, which resulted in a three-layer model of p-wave velocities of $v_1 = 320\text{--}370\text{ m s}^{-1}$, $v_2 = 790\text{--}820\text{ m s}^{-1}$ and $v_3 = 3200\text{--}3300\text{ m s}^{-1}$ (Figure 3). The first refractor was identified at depths between 1 and 2.5 m. The second refractor is located at depths between 3.5 and 4 m but is shallower towards the east (Figure 3). The velocity model was checked by network raytracing techniques which resulted, after careful modification of the initial model, in a total absolute time difference of 0.79 ms and a total time difference of -0.45 ms between measured and calculated travel times. Thus, the depths of refractors in the model could be slightly greater than the real depths. Weather conditions did not allow us to collect offset-shots or shots between geophones, so the horizontal trend of refractors should be interpreted with caution. However, we observed a sharp p-wave velocity rise at the second refractor, which was detected at depths of 3.5–4 m.

GPR

Before conducting the GPR surveys (Figure 2), we made CMP measurements. CMP data allow calculation of the speed of electromagnetic waves, which can be also used to identify reflective horizons. We chose fairly flat, vegetated

and smooth parts of the rock glacier surface but not all surveys yielded good results because the size of boulders on and within the upper layers of the rock glacier are from 0.5 to >2 m in diameter. These boulders can prevent full contact of the antennae with the ground or cause unwanted diffraction signals during CMP measurements (Jol and Bristow, 2003). At the chosen location, velocity analysis shows a velocity of 0.11 m ns^{-1} for the upper 4 m, and a velocity reduction down to 0.065 m ns^{-1} between 4 and 4.8 m (Figure 4). At about 100 ns, the velocity rises sharply to 0.152 m ns^{-1} . Below 110 ns, no usable hyperbolas could be identified in the CMP file. The CMP analyses are consistent with the observed change of reflections and velocity estimates using diffraction hyperbolas except for the 0.8-m thick zone of low velocity, which is not discernible at a frequency of 50 MHz.

Several GPR lines were collected along and across the rock glacier but only GPR-1 is treated here because it yielded the best data quality. GPR-1 starts at the toe of the talus and extends 125 m along the axis of the western lobe (Figure 2). The radar image shows an undulating reflection zone parallel to the surface which starts between 60 and 100 ns (zone a in Figure 5) followed by a zone with less clear reflections and low amplitudes (cf. Berthling *et al.*, 2003). From 0–16 m and 120–300 ns an oblique reflection

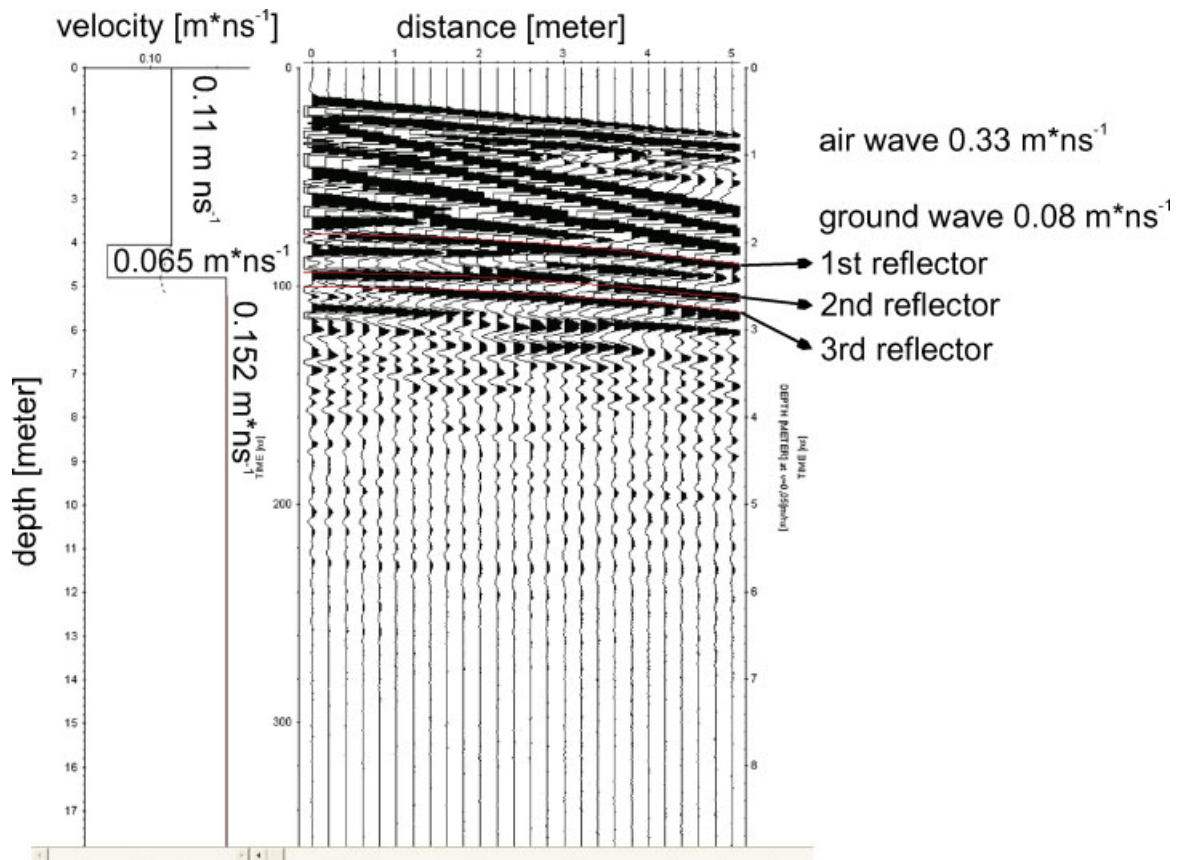


Figure 4 Common midpoint survey plot with one-dimensional velocity analysis conducted with 100-MHz antennae. Note the sharp rise in velocity at 100 ns (approximately 4.7 m). This figure is available in colour online at wileyonlinelibrary.com

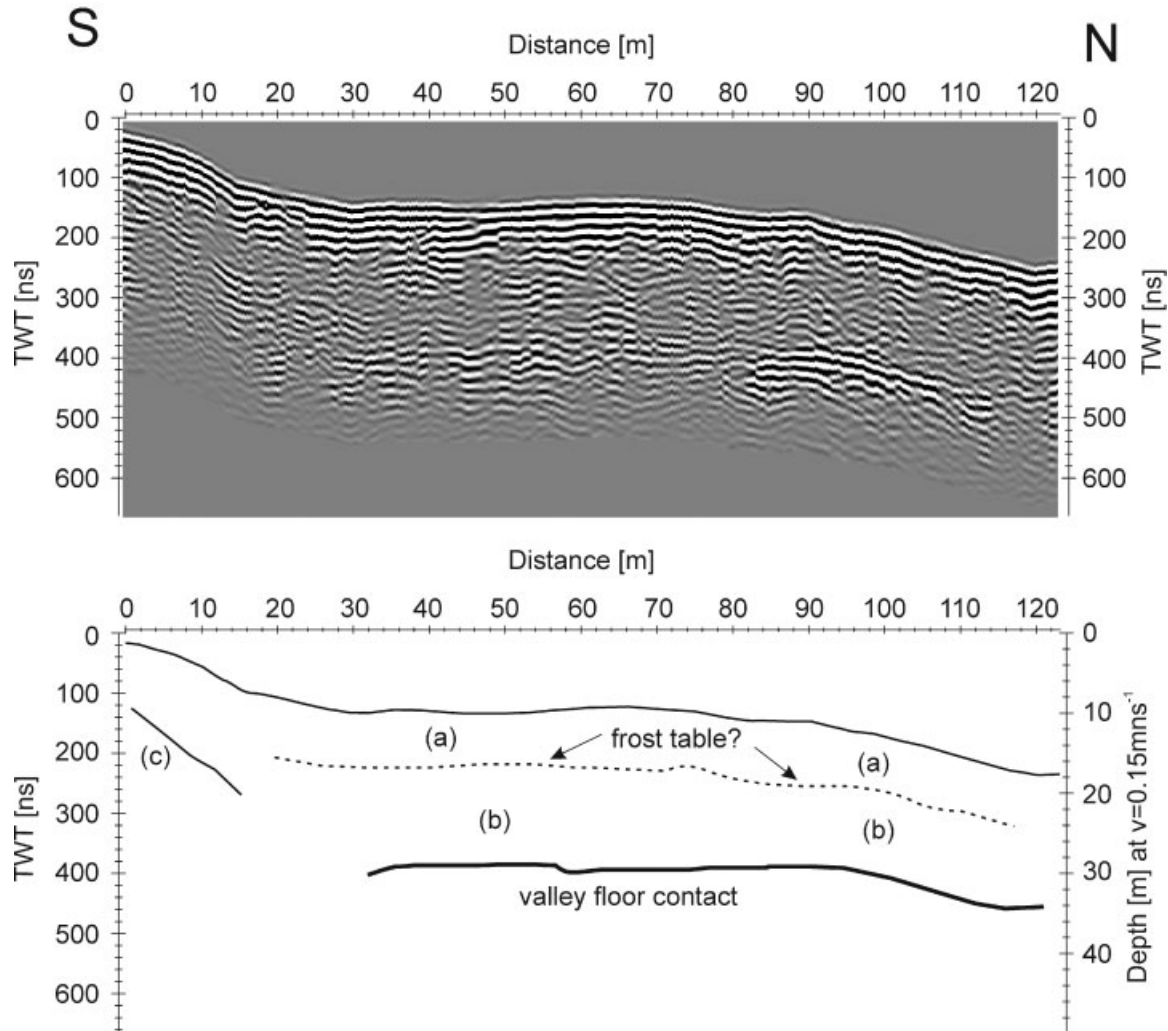


Figure 5 Image of Green Lake 5 rock glacier ground-penetrating radar (GPR) 1 after application of the filter sequence and topography correction in the upper part and an outline of the most prominent reflections in the lower part of the figure. Note the prominent reflection of the valley-floor contact at the base of the 50-MHz GPR image. TWT = Two-way travel time. (a), (b) and (c) reflect major stratigraphic units.

is evident (zone c). A prominent high-amplitude reflection is most clearly developed between 85 and 115 m and can be traced to the south and north from there.

ERT

The ERT models of the two profiles on the rock glacier (Figure 2, RG-Tomo-1 and RG5-Tomo-2) show a wide range of specific resistivities, from 1 k Ω m to >300 k Ω m. The specific resistivities of both profiles can be grouped into four layers (Figure 6). In the upper 0.7 to 1 m the lines show a zone of 0 to 10–20 k Ω m. This zone is especially well developed along RG5-Tomo-1 but is also partly evident on RG-Tomo-2. Below it is a layer that extends from about 1 m down to 2–3-m depth and is characterised by resistivity values from 20–30 k Ω m to 100 k Ω m. At the beginning of RG5-Tomo-2 this layer is up to 5–6 m thick. Below the second layer a well-developed third layer is visible. It starts at a depth

of 1–3 m depending on the line, and extends down to about 4–5 m on average and reaches a maximum depth of 6 m at RG5-Tomo-2 between 16 and 32 m along the line. Layer three is characterised by specific resistivities of 5–20 k Ω m. Finally, both lines exhibit a fourth layer which starts 5–6 m below the surface and yields resistivity values of >50 k Ω m.

The DOI index clearly documents the high quality of the data (Figure 6) as the calculated inversions are reliable through most of the model. Only below the high-resistivity areas of the upper 1–2 m at RG5-Tomo-1 and -2 and in the deepest parts of the profiles is the calculated DOI index above 0.2. In these areas, the interpretation should be treated as tentative as these regions of the model are not very well constrained by the data (Hilbich *et al.*, 2009). However, the main transition from lower to much higher specific resistivities at about 5-m depth is within the 0.1 DOI range and so the data appear to constrain the model (Oldenburg and Li, 1999).

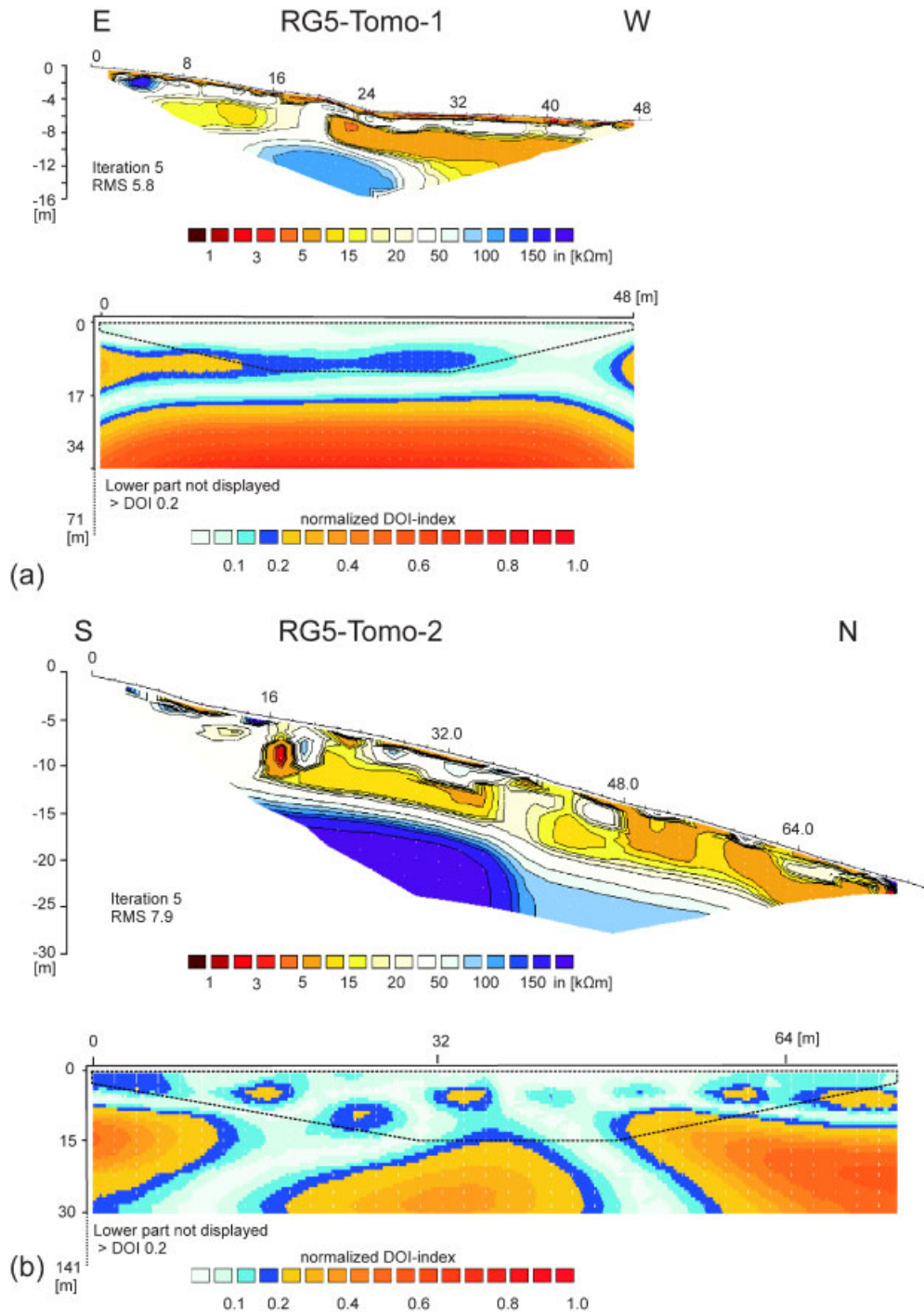


Figure 6 Inversion results of electrical resistivity tomography images from (a) Green Lake 5 rock glacier (RG5) Tomo-1 and (b) RG5-Tomo-2. The calculation of the normalised depth of investigation (DOI) index is given below each inversion. The line in the DOI index images outlines the area of data for each line. Hilbich *et al.* (2009) suggest a threshold value of 0.2 for the DOI index which here is indicated by the transition from dark blue to orange colours. This figure is available in colour online at wileyonlinelibrary.com

INTERPRETATION

Here we take the physical values of each method, discuss them in relation to values that are characteristic for different

materials and compare them to values obtained from other studies or from the laboratory.

The p-wave velocity model for RG5-SSR-1 on the rock glacier shows two refractors. As the seismic line extended

across an area with grassy vegetation, the first two layers most likely represent unconsolidated sediment and soil overlying a layer with higher compaction or larger boulders (Figure 3, layer S1 = 320–370 m s⁻¹, S2 = 790–820 m s⁻¹). The velocity and interpretation of layer S2 is similar to the results of our study of slope deposits nearby on Niwot Ridge where materials were characterised as a mixture of periglacially derived rock fragments, boulders and fines (Leopold *et al.*, 2008b). However, the observed rise in velocity could also indicate a zone with higher water content and thus a higher velocity. At the second refractor the seismic velocity rises sharply to $v_3 = 3200\text{--}3300\text{ m s}^{-1}$ (layer S3 in Figure 3). Such high velocities are typical of bedrock or ice-cemented sediments (Hauck and Kneisel, 2008; Ikeda, 2008). Bedrock at a depth of only 4 m (i.e. well above that exposed on the adjacent valley floor) seems unrealistic and so we interpret layer three as a zone of frozen debris and ice. Hausmann *et al.* (2007) suggested that a velocity less than that of pure ice at 0°C ($\sim 3750\text{ m s}^{-1}$) indicates a reduction of the solid (frozen) contacts between ice and boulders within the ice core and the formation of a water film along these contacts. Increased amounts of air can also cause lower p-wave velocities.

In general, the CMP velocity sounding by GPR corroborates the results of the seismic survey. The electromagnetic signal travels through the upper 4-m thick zone with a velocity of 0.11 m ns⁻¹, which we interpret as boulders and debris with open pores and few fines between the clasts, consistent with other studies (Hauck and Kneisel, 2008, p. 236). The velocity is greater than that measured in periglacial slope deposits on Niwot Ridge, which yielded values of 0.09 m ns⁻¹ in the blocky unfrozen layer (Leopold *et al.*, 2008b). This difference may result from larger boulders and a higher proportion of air between the boulders on RG5. From about 90–100 ns we observed a velocity reduction to 0.065 m ns⁻¹ in a second zone, which is interpreted as an abrupt change in water content distribution within the rock glacier. A water-rich mixed zone that is developed within silty-sand fines would be characteristic of the lower active layer, near the thaw front, as reported by other authors (Haerberli *et al.*, 2006). Velocities of 0.06 m ns⁻¹ for the active layer have also been reported in other studies (e.g. Berthling and Melvold, 2008). On RG5, the velocity of the deepest reflector was 0.15 m ns⁻¹, which is characteristic of ice rich-debris. It is consistent with the velocity range of 0.14 to 0.15 m ns⁻¹ described in other studies (Schmöllner and Fruhwirth, 1996; Isaksen *et al.*, 2000; Lehmann and Green, 2000; Berthling *et al.*, 2003; Hausmann *et al.*, 2007). Pure ice has an electromagnetic wave speed of about 0.168 m ns⁻¹ (e.g. Davis and Annan, 1989; Eisen *et al.*, 2002), a level we did not observe at RG5. Fukui *et al.* (2008) describe a velocity of 0.17 m ns⁻¹ in a rock glacier with a pure ice core that was interpreted as a glacier-derived feature. The low-amplitude zone in our GPR image (zone b in Figure 5) corresponds with observations by Berthling *et al.* (2000), who described such a zone as a relatively ice-rich

layer. However, later Berthling *et al.* (2003) interpreted this low-amplitude zone partly as an effect of the applied automatic gain control (AGC)-gain function. We used a linear gain with low values for the upper layers and a stronger gain at greater depth. Therefore we interpreted the basal/low-amplitude zone as a less reflective zone due to a high ice content. The prominent reflection at the base of the radar image has a depth of about 18 m, which may correspond to the total thickness of the rock glacier at this site.

The inversion results of the apparent electrical resistivities on the upper subsurface of RG5 (Figure 6a and b) show a very shallow zone with low resistivity on top (RG5-R1 in Figure 7a), interpreted as soils and fine sediments, followed by a zone characterised by higher specific resistivities up to 50 kΩm (RG5-R2) due to possible air spaces and a 2–3-m thick layer with about 5–20 kΩm (RG5-R3). We interpret these three layers as the heterogeneous structure of the active layer on RG5. In general, it is consistent with our interpretation from the SSR and GPR surveys but layer thicknesses vary. With increasing depth, resistivity values rise again to >50 kΩm, reaching values of >150 kΩm (RG5-R4 in Figure 7a). Based on the resistivities, we interpret this fourth zone as an ice-rich permafrost zone, possibly a pure ice body, within the rock glacier. Unfortunately, we did not measure any diffraction hyperbola from our GPR survey at this depth, which would have allowed us to distinguish between pure ice and ice-rich debris.

A MODEL FOR THE INTERNAL STRUCTURE OF RG5

The results of the geophysical surveys were integrated into a model of RG5 (Figure 7a). This includes layers and their boundaries as well as the range of data from the three methods. The geophysical model was converted into a stratigraphic model of the internal structure of RG5 (Figure 7b). It starts with fine sediments and soils at the surface overlying a zone of coarse debris containing large air-filled voids, which extends to about 2–3-m depth. Between 1–3- and 4–5-m depth, we suggest a change in materials to finer and wetter sediments that are unfrozen in late summer. This zone corresponds to the lowest part of the active layer during the climatic conditions of recent years. Below 4–5 m, GPR signals and ERT images both suggest a fourth zone within the rock glacier body that is best interpreted as debris with a very high ice content. The data provide only weak indications of a solid ice core in RG5, but we recognise that they have less explanatory power with increasing depth. Nevertheless, bedrock could be detected at a depth of about 16–18 m and this is consistent with its exposure on the adjacent valley floor.

Williams *et al.* (2006) hypothesised that the rock glacier has an internal ice core surrounded by interstitial ice within coarse debris. They suggested that the 0°C isotherm was

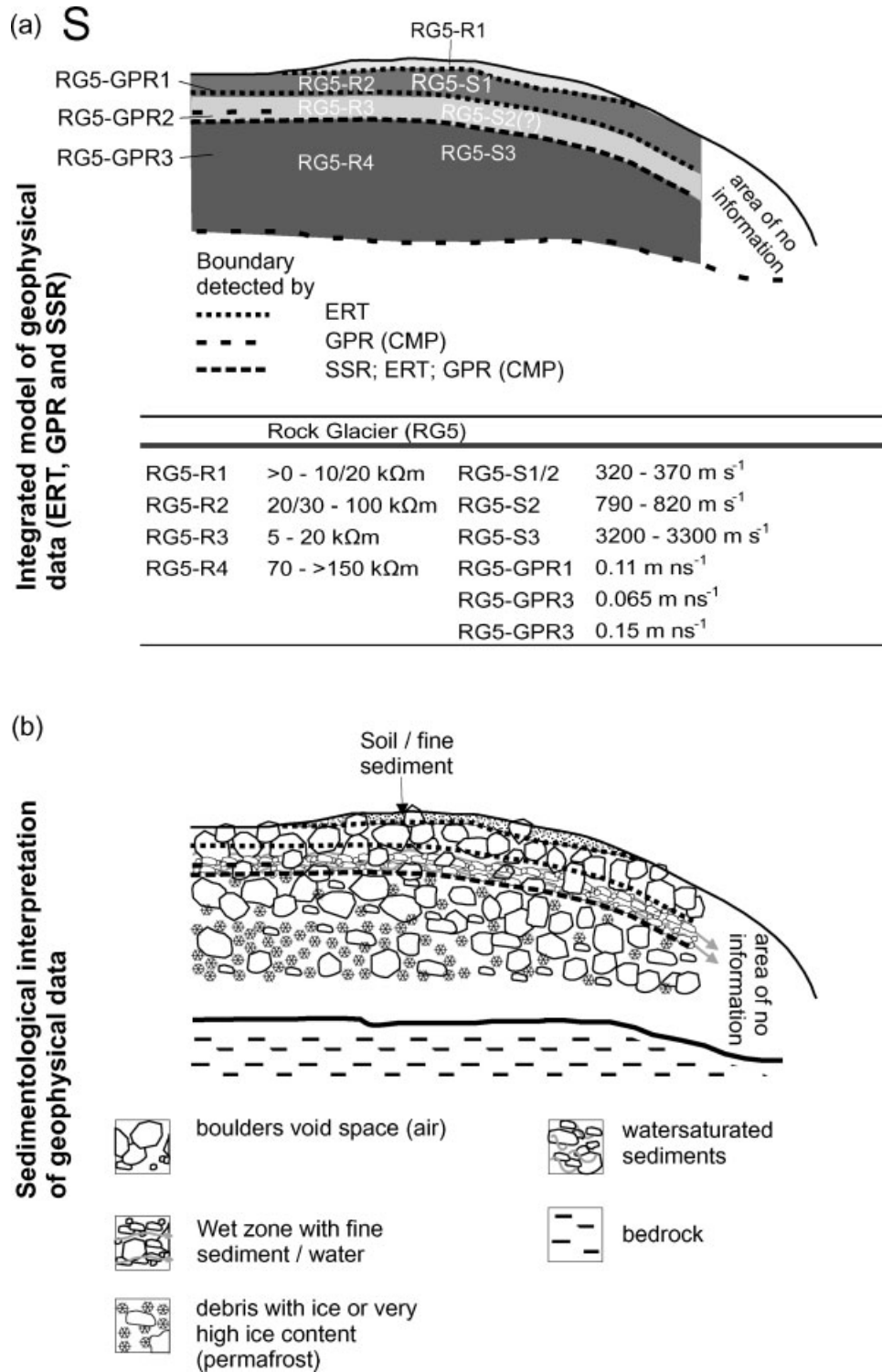


Figure 7 (a) Integrated model of the Green Lake 5 rock glacier (RG5) based on the three geophysical methods and (b) interpreted sedimentological model of the internal structure of the rock glacier. GPR = Ground-penetrating radar; ERT = electrical resistivity tomography; SSR = shallow seismic refraction; CMP = common midpoint.

near the surface of the rock glacier at the start of snowmelt and extended deeper during the summer as the active layer thawed. They further speculated that in early summer water percolating through large voids in the rock glacier travels rapidly, resulting in low residence times. Hydrologic mixing models parameterised with stable water isotopes and geochemical tracers suggested that water flow at this time was primarily 'new' water from that year's snowmelt, which has little opportunity to react with the debris and so has low solute concentrations. In autumn, the 0°C isotherm reaches the interstitial ice, some of which is melted, and residence times are greater, providing a baseflow with much higher solute content.

In general, the geophysical model is consistent with the hydrologic one but it adds information on the types of sediments, their stratigraphy and thickness. Both models start with the fine-grained material and soils visible at the surface of the rock glacier. Williams *et al.* (2007) showed that this surface layer was the site of active biogeochemical processes such as the mineralisation of organic matter. We now know that this layer of 'soil-like' texture reaches a maximum depth of 0.5–1 m. It is absent on the neighbouring talus and is less evident at the sides and fronts of the two lobes. Furthermore, it is less extensive on the western lobe, which moves with a slightly higher velocity.

A coarse, blocky material with air-filled interstices is found below the thin surface layer, which it breaks in places. These large void spaces potentially allow Balch circulation to facilitate seasonal freezing, a rapid water flux between the uppermost soil cover down to the lower permeability zone 3, the third layer of Figure 3, and equally rapid lateral flow above the low-permeability zone. This supports the inference of a low residence time of infiltrating water in the rock glacier during the summer months (Williams *et al.*, 2006). During our geophysical surveys we detected a 1–3 m-thick wet zone in the lower part of the active layer where voids seem to be filled with fines and liquid water. The lower part of this zone represents the location of the 0°C isotherm at the time of observation. The geophysical model suggests an active-layer depth at the end of the melt season that is between 4 and 5 m and even deeper in some areas.

CONCLUSION

Our geophysical surveys support the stratigraphy and structure of RG5 inferred by Williams *et al.* (2006) on the basis of water-quality observations. They add important quantitative information to Williams *et al.*'s (2006) model, defining the vertical depth of important thresholds in the structure such as the depth of the active layer within the rock glacier during late summer. The active layer on the rock glacier is between 4 and 5 m deep, which is greater than estimates for fine-rich slope sediments in nearby areas of Niwot Ridge (e.g. Ives, 1973; Leopold *et al.*, 2008a).

It proved important to employ multiple geophysical techniques in order to maximise the strength of each method and minimise their limitations (Hauck and Kneisel, 2008; Schrott and Sass, 2008). The blocky surface of the rock glacier sets made the acquisition of some geophysical data challenging. However, a multiple approach reduced the ambiguities inherent in indirect geophysical methods in order to provide a fully interpretable and detailed geophysical model.

A basic knowledge of the internal structure of rock glaciers is vital if we want to increase our understanding of landform dynamics and sensitivity to climatic conditions. We also need information about spatio-temporal changes within the rock glacier but to date most studies have used geophysical methods on a single occasion. Recent improvements in technology have made it feasible to use geophysical methods such as ERT on a continuous basis and we plan to establish such a monitoring system at RG5.

ACKNOWLEDGEMENTS

The research was carried out under the funding framework of the BC-CZO sponsored by the US National Science Foundation (NSF-0724960). Logistical support and data were kindly provided by the NSF-supported Niwot Ridge LTER project (DEB-0423662) and the University of Colorado Mountain Research Station. We thank Craig Skeie, Water Resources Facility Manager of the City of Boulder watershed, for his help. We are grateful for constructive comments given by O. Sass and a second anonymous reviewer. We also thank A. Lewkowicz for comments and editing.

REFERENCES

- Azócar GF, Brenning A. 2010. Hydrological and geomorphological significance of rock glaciers in the Dry Andes, Chile (278-338S). *Permafrost and Periglacial Processes* **21**: 42–53. DOI: 10.1002/ppp.669.
- Barsch D. 1996. *Rockglaciers*. Springer-Verlag: Berlin; 331pp.
- Berthling I, Melvold K. 2008. Ground-penetrating radar. In *Applied Geophysics in Periglacial Environments*, Hauck C, Kneisel C (eds). Cambridge University Press: New York; 81–97.
- Berthling I, Etzelmüller B, Isaksen K, Sollid J. 2000. Rock Glaciers on Prins Karls Forland. II: GPR Soundings and the Development of Internal Structures. *Permafrost and Periglacial Processes* **11**: 357–369. DOI: 10.1002/1099-1530(200012)11:4<357::AID-PPP366>3.0.CO;2-6.
- Berthling I, Etzelmüller B, Wale M, Sollid JL. 2003. Use of Ground Penetrating Radar (GPR) soundings for investigating internal structures in rock glaciers. Examples from Prins Karls Forland, Svalbard. *Zeitschrift für Geomorphologie Supplement* **132**: 103–121.
- Brenning A, Azócar GF. 2010. Statistical Analysis of Topographic and Climatic Controls and Multispectral Signatures of Rock Glaciers in the Dry Andes, Chile (278-338S). *Permafrost and Periglacial Processes* **21**: 54–66. DOI: 10.1002/ppp.670.
- Caine N. 1996. Streamflow patterns in the alpine environment of North Boulder Creek, Colorado Front Range. *Zeitschrift für Geomorphologie* **104**: 27–42.

- Caine N. 2001. Geomorphic systems of Green Lakes Valley. In *Alpine Dynamics: The Structure and Function of an Alpine Ecosystem: Niwot Ridge, Colorado*, Bowman W, Seastedt TR (eds). Oxford University Press: Oxford; 45–74.
- Clow D, Schrott L, Webb R, Campbell D, Torizzo A, Dornblaser M. 2003. Ground water occurrence and contributions to streamflow in an alpine catchment, Colorado Front Range. *Ground Water* **41**(7): 937–950. DOI: 10.1111/j.1745-6584.2003.tb02436.x.
- Corte A. 1976. The hydrological significance of rock glaciers. *Journal of Glaciology* **17**(75): 157–158.
- Davis J, Annan A. 1989. Ground-penetrating radar for high resolution mapping of soil and rock stratigraphy. *Geophysical Prospecting* **37**: 531–551. DOI: 10.1111/j.1365-2478.1989.tb02221.x.
- Degenhardt J. 2009. Development of tongue-shaped and multilobate rock glaciers in alpine environments – Interpretations from ground penetrating radar surveys. *Geomorphology* **109**: 94–107. DOI: 10.1016/j.geomorph.2009.02.020.
- Degenhardt J, Giardino J, Junck M. 2003. GPR survey of a lobate rock glacier in Yankee Boy Basin, Colorado, USA. In *Ground Penetrating Radar in Sediments*, Bristow C, Jol H (eds). Geological Society: London; Special Publication 211: 167–179. DOI: 10.1144/GSL.SP.2001.211.01.14.
- Eisen E, Nixdorf U, Wilhelms F, Miller H. 2002. Electromagnetic wave speed in polar ice: Validation of the CMP technique with high-resolution dielectric profiling and γ -density measurements. *Annals of Glaciology* **34**: 150–156. DOI: 10.3189/172756402781817509.
- Fukui K, Sone T, Strelin J, Torielli C, Mori J, Fujii Y. 2008. Dynamics and GPR stratigraphy of a polar rock glacier on James Ross Island, Antarctic Peninsula. *Journal of Glaciology* **54**(186): 445–451. DOI: 10.3189/002214308785836940.
- Greenland D. 1989. The climate of Niwot Ridge, Front Range, Colorado, U.S.A. *Arctic and Alpine Research* **21**(4): 380–391.
- Haeberli W, Hallet B, Arenson L, Elcönin R, Humlum O, Kääh A, Kaufmann V, Ladanyi B, Matsuoka N, Springman S, Vonder Mühll D. 2006. Permafrost Creep and Rock Glacier Dynamics. *Permafrost and Periglacial Processes* **17**: 189–214. DOI: 10.1002/ppp.561.
- Harris C, Vonder Mühll D, Isaksen K, Haeberli W, Sollid JL, King L, Holmlund P, Dramis F, Guglielmin M, Palacios D. 2003. Warming permafrost in European mountains. *Global and Planetary Change* **39**(3-4): 215–225. DOI: 10.1016/j.gloplacha.2003.04.001.
- Harris C, Arenson L, Christiansen H, Eitzmüller B, Frauenfelder B, Gruber S, Haeberli W, Hauck C, Hölzle M, Humlum O, Isaksen K, Kääh A, Kern-Lütschg M, Lehning M, Matsuoka N, Murton J, Nötzli J, Phillips M, Ross N, Seppälä M, Springman S, Vonder Mühll D. 2009. Springman S and Vonder Mühll D. 2009. Permafrost and climate in Europe: Monitoring and modelling thermal, geomorphological and geotechnical responses. *Earth-Science Reviews* **92**: 117–171. DOI: 10.1016/j.earscirev.2008.12.002.
- Hauck C, Kneisel C. 2008. *Applied Geophysics in Periglacial Environments*. Cambridge University Press: Cambridge; 240pp.
- Hauck C, Vonder Mühll D. 2003. Inversion and interpretation of Two-dimensional Geoelectrical Measurements for detecting Permafrost in Mountain Regions. *Permafrost and Periglacial Processes* **14**: 305–318. DOI: 10.1002/ppp.462.
- Hausmann H, Krainer K, Brückl E, Mostler W. 2007. Internal structure and ice content of Reichenkar rock glacier (Stubai Alps, Austria) assessed by geophysical investigations. *Permafrost and Periglacial Processes* **18**(4): 351–367. DOI: 10.1002/ppp.601.
- Hilbich C, Marescot L, Hauck C, Loke M, Mäusbacher R. 2009. Applicability of Electrical Resistivity Tomography Monitoring to Coarse Blocky and Ice-rich Permafrost Landforms. *Permafrost and Periglacial Processes* **20**: 269–284. DOI: 10.1002/ppp.652.
- Hoffmann T, Schrott L. 2003. Determining sediment thickness of talus slopes and valley fill deposits using seismic refraction – a comparison of 2D interpretation tools. In *Geophysical Applications in Geomorphology*, Schrott L, Hördt A, Dikau R (eds). Zeitschrift für Geomorphologie, N.F., Supplement 132: 71–87.
- Ikeda A. 2008. Reassessment of DC resistivity in rock glaciers by comparing with P-wave velocity: a case study in the Swiss Alps. In *Applied Geophysics in Periglacial Environments*, Hauck C, Kneisel C (eds). Cambridge University Press: Cambridge; 137–152.
- Isaksen K, Ødegard R, Eiken T, Sollid J. 2000. Composition, flow and development of two tongue-shaped rock glaciers in the permafrost of Svalbard. *Permafrost and Periglacial Processes* **11**: 241–257. DOI: 10.1002/1099-1530(200007/09)11:3<241::AID-PPP358>3.0.CO;2-A.
- Ives JD. 1973. Permafrost and its relationship to other environmental parameters in a midlatitude, high altitude setting, Front Range, Colorado Rocky Mountains. In *Permafrost: The North American Contribution to the 2nd International Conference*. National Academy of Science, Washington, DC: 121–125.
- Janke J. 2005. The occurrence of alpine permafrost in the Front Range of Colorado. *Geomorphology* **67**: 375–389. DOI: 10.1016/j.geomorph.2004.11.005.
- Janke J. 2007. Colorado Front Range Rock Glaciers: Distribution and Topographic Characteristics. *Arctic, Antarctic and Alpine Research* **39**(1): 74–83. DOI: 10.1657/1523-0430(2007)39[74:CFRRGD]2.0.CO;2.
- Jol H, Bristow C. 2003. GPR in sediments: a good practice guide. In *Ground Penetrating Radar in Sediments*, Bristow C, Jol H (eds). Geological Society: London; Special Publication 211: 9–27. DOI: 10.1144/GSL.SP.2001.211.01.02.
- Kneisel C, Hauck C, Fortier R, Moorman B. 2008. Advances in Geophysical Methods for Permafrost Investigations. *Permafrost and Periglacial Processes*, **16**: 157–178. DOI: 10.1002/ppp.616.
- Krainer K, Mostler W. 2002. Hydrology of active rock glaciers: examples from the Austrian Alps. *Arctic, Antarctic, and Alpine Research* **34**(2): 142–149.
- Krummel H. 2005. Seismische Quellen. In *Handbuch zur Erkundung des Untergrundes von Deponien und Altlasten*, Knödel K, Krummel H, Lange G (eds). 3: 467–504.
- Lehmann F, Green AG. 2000. Topographic migration of georadar data: Implications for acquisition and processing. *Geophysics* **65**(3): 836–848. DOI: 10.1190/1.1444781.
- Leopold M, Dethier D, Völkel J. 2008a. Shape, thickness and distribution of periglacial slope deposits at Niwot Ridge, Rocky Mountains Front Range, Colorado, USA. *Zeitschrift für Geomorphologie N.F. 52 Supplement 2*: 77–94.

- Leopold M, Dethier D, Völkel J, Raab T, Corson-Rickert T, Caine N. 2008b. Using geophysical methods to study the shallow subsurface at a sensitive alpine site, Niwot Ridge, Colorado Front Range, USA. *Arctic, Antarctic and Alpine Research* **40**(3): 519–530. DOI: 10.1657/1523-0430(06-124).
- Leopold M, Voelkel J, Dethier D, Williams M, Caine N. 2010. Mountain Permafrost – a valid archive to study climate change? Examples from the Rocky Mountains Front Range of Colorado, USA. *Nova acta Leopoldina* **112**: 281–289.
- Li X, Cheng G, Jin H, Kang E, Che T, Jin R, Wu L, Nan Z, Wang J, Shen Y. 2008. Cryospheric Change in China. *Global and Planetary Change* **62**: 210–218. DOI: 10.1016/j.gloplacha.2008.02.001.
- Loke M, Barker R. 1995. Least-squares deconvolution of apparent resistivity. *Geophysics* **60**(6): 1682–1690. DOI: 10.1190/1.1443900.
- Marescot L, Loke M, Chapellier D, Delaloye R, Lambiel C, Reynard E. 2003. Assessing reliability of 2D resistivity imaging in mountain permafrost studies using the depth of investigation index method. *Near Surface Geophysics* **1.2**: 57–67.
- Maurer H, Hauck C. 2007. Geophysical imaging of alpine rock glaciers. *Journal of Glaciology* **53**(180): 110–120. DOI: 10.3189/172756507781833893.
- Millar C, Westfall R. 2008. Rock glaciers and related periglacial landforms in the Sierra Nevada, CA, USA; inventory, distribution and climatic relationships. *Quaternary International* **188**: 90–104. DOI: 10.1016/j.quaint.2007.06.004.
- Neal A. 2004. Ground-penetrating radar and its use in sedimentology: principles, problems and progress. *Earth-Science Reviews* **66**: 261–330. DOI: 10.1016/j.earscirev.2004.01.004.
- Oldenburg D, Li Y. 1999. Estimating depth of investigation in DC resistivity and IP surveys. *Geophysics* **64**: 403–416. DOI: 10.1190/1.1444545.
- Outcalt S, Benedict J. 1965. Photointerpretation of two types of rock glacier in the Colorado Front Range, U.S.A. *Glaciology* **5**: 849–856.
- Schmöller R, Fruhwirth R. 1996. Komplex-geophysikalische Untersuchungen auf dem Dösener Blockgletscher (Hohe Tauern, Österreich). Beiträge zur Permafrostforschung in Österreich, Graz, Band **33**.
- Schrott L, Sass O. 2008. Application of field geophysics in geomorphology: Advances and limitations exemplified by case studies. *Geomorphology* **93**: 55–73. DOI:10.1016/j.geomorph.2006.12.024.
- White S. 1971. Rock glacier studies in the Colorado Front Range, 1961 to 1968. *Arctic & Alpine Research* **3**: 43–64.
- White S. 1976. Rock glaciers and Block Fields, Review and New Data. *Quaternary Research* **6**: 77–97.
- White S. 1981. Alpine mass movement forms (noncatastrophic): classification, description, and significance. *Arctic and Alpine Research* **13**(2): 127–137.
- Williams M, Losleben M, Caine N, Greenland D. 1996. Changes in climate and hydrochemical responses in a high-elevation catchment, Rocky Mountains. *Limnology and Oceanography* **41**(5): 939–946.
- Williams M, Knauf M, Caine N, Liu F, Verplanck P. 2006. Geochemistry and Source Waters of Rock Glacier Outflow, Colorado Front Range. *Permafrost and Periglacial Processes* **17**: 13–33. DOI: 10.1002/ppp.535.
- Williams M, Knauf M, Cory R, Caine N, Liu F. 2007. Nitrate Content and Potential Microbial Signature of Rock Glacier Outflow, Colorado Front Range. *Earth Surface Processes and Landforms* **32**: 1032–1047. DOI: 10.1002/esp.1455.